



## Joys and sorrows of FEM with strong discontinuities for the variational approximation of free- discontinuity problems

M. Angelillo

*Department of Civil Engineering, University of Salerno, Fisciano (SA) (Italy)*  
*mangelillo@unisa.it*

E. Babilio

*Department of Applied Mathematics and Structural Mechanics, University of Napoli – Federico II, Napoli (Italy)*  
*ebabili@hotmail.com*

A. Fortunato

*Department of Civil Engineering, University of Salerno, Fisciano (SA) (Italy)*  
*a.fortunato@unisa.it*

---

**ABSTRACT.** In the present paper we consider a numerical method for Variational Fracture based on classical finite elements with gaps, the novelty being the way in which the FE mesh is moved to approximate the cracks. Indeed VF requires the ability to locate and approximate the crack fronts. On adopting the discrete, “strong discontinuity” approach cracks cannot be restricted to the skeleton of a fixed FE mesh. With our method mesh is made variable: mesh nodes are taken as further unknowns and the minimization of the Energy is considered, at the same time, with respect to displacements and positions of the nodes of the mesh in the reference configuration (minimization over variable triangulations).

The results we present are still of a research type. To simplify the computations, the mesh we adopt are still too coarse to accurately catch the large values of the gradient of displacement that arise at the crack tips and so the energy. Also the descent strategy we use to solve the variational problem, though the most natural, is numerically rather slow.

The issue we try to address here is to verify the possibility of tracking cracks by using FE with gaps, without resorting to sophisticated numerical tools, by working on simple benchmark problems.

**SOMMARIO.** In questo lavoro si presenta un metodo numerico per l'approssimazione di problemi di Frattura variazionale, basato su elementi finiti classici con discontinuità finite. La novità del metodo risiede nel modo in cui la mesh si adatta per approssimare le fratture. Adottando l'approccio discreto, le fratture non possono essere ristrette allo scheletro di una mesh fissa. Con il nostro metodo la mesh è resa variabile (ed adattabile) considerando la posizione dei nodi della mesh come un'ulteriore variabile, la minimizzazione dell'energia si effettua allo stesso tempo rispetto alla variazione degli spostamenti e delle coordinate dei nodi della mesh nella configurazione di riferimento (minimizzazione su triangolazioni variabili).

I risultati che presentiamo sono ancora preliminari, in quanto per contenere i tempi di computazione, la mesh che si adotta è piuttosto rada per essere in grado di rappresentare accuratamente i forti gradienti che sono presenti all'apice della frattura e, di conseguenza, l'energia del sistema. Anche la strategia di discesa che adottiamo per ottenere le soluzioni di minimo, sebbene la più naturale, è notoriamente lenta.

L'obiettivo qui è mostrare la possibilità di individuare e tracciare le fratture utilizzando elementi finiti con discontinuità forti, senza ricorrere a strumenti numerici sofisticati e lavorando su esempi di complessità limitata.

---



**KEYWORDS.** Griffith criterion; Variational fracture; Fracture tracking; Strong discontinuities.

## INTRODUCTION

The complexity of fracture nucleation and propagations in engineering applications calls for efficient numerical methods of analysis. Finite element methods are used extensively in Griffith's type linear elastic fracture mechanics. The most commonly used FE models are the virtual crack closure technique (Krueger [1]) and, more recently the Extended Finite Element Method (X-FEM, Moës, Dolbow, Belitschko [2]). These approaches represent cracks as discrete strong discontinuities, either by remeshing and inserting discontinuity lines, or by enriching the shape functions inside the elements with discontinuous components. Tracking the evolution of complex fracture lines (surfaces) has proven to be a hard task with both approaches.

Alternative methods for the numerical simulation of brittle fracture are the phase fields approach and other regularization methods invented for the numerical handling of free-discontinuity problems, such as Variational Fracture (Ambrosio-Tortorelli [3]). In the last decade VF has emerged as a new point of view of an old, successful theory: namely the Griffith's energy criterion for crack propagation. With VF energy convenience determines not only "when" the fracture should nucleate or propagate, but also the "how", that is which are the optimal paths the cracks choose to follow. With such methods the fracture line (surface) is approximated by a phase field which smoothes the crack line (surface) over a small strip (snake). This method has been recently extended to dynamics (Larsen [4]) and very recent numerical results (Borden et al. [5]) confirm the anticipation that phase fields methods could be particularly efficient when branching or merging of cracks occur in 2d or 3d applications.

Phase field methods still require almost uniform meshes and extremely fine mesh sizes to accurately reproduce the crack front (roughly  $10^{-4}$  of the overall dimensions of the body). This makes, at the moment, difficult for the phase field approach the implementation into commercial codes.

In the present paper we consider a numerical method for VF based on classical finite elements with gaps, the novelty being the way in which the FE mesh is moved to approximate the cracks. Indeed VF requires the ability to locate and approximate the crack fronts. On adopting the "strong discontinuity" approach cracks cannot be restricted to the skeleton of a fixed FE mesh. With our method mesh is made variable: mesh nodes are taken as further unknowns and the minimization of the Energy is considered, at the same time, with respect to displacements and positions of the nodes of the mesh in the reference configuration (minimization over variable triangulations).

The results we present are still of a research type, since no attempt has been made to improve the efficiency of the numerical method, by optimizing the balance between the number of unknowns and the mesh size. The mesh we adopt are still too coarse to accurately catch the large values of the gradient of displacement that arise at the crack tips and also the descent strategy we use to solve the variational problem, though the most natural, is numerically rather slow.

The issue we try to address here is to verify the possibility of tracking cracks by using FE with gaps, without resorting to sophisticated numerical tools. To render the method numerically efficient both the time and space discretization should be optimized by introducing highly localized refinement capabilities and may be resorting to different minimization strategies (such as staggered ("two step") minimization: first w.r. to displacement and then w.r. to mesh).

With a Griffith type interface energy fracture nucleation is always brutal: descent directions for the energy do not exist in absence of singularities (such as a pre-existing crack) or, if a singularity is present, but the problem is approximated via FE. To reach more energetically convenient local minima the system must have the ability to surmount small energy barriers. The strategy we adopt to smooth out these wells is a form of relaxation of the interface energy. Such a relaxation corresponds to the introduction of a sort of fictitious cohesive-type model in a way similar to what is done with the phase fields approaches.

## PRELIMINARIES

Consider a two-dimensional body  $\mathcal{B}$  occupying in the original configuration a bounded plane domain  $\Omega$  and undergoing small deformations in the time interval  $T$ . Let  $\boldsymbol{\varepsilon}$  be the infinitesimal strain field and  $\mathbf{u}$  the displacement field both defined over  $\Omega \times T$ . The boundary of  $\Omega$  is partitioned into two parts where displacements  $\mathbf{u}$  and



tractions  $\mathbf{p}$  are given. These boundary conditions are generally time dependent in the given time interval  $T$ .

We admit that  $\mathbf{u}$  may be discontinuous on a set  $\Gamma$  assumed to belong to an admissible set of cracks  $\mathcal{S}(\Gamma)$ . The crack pattern

$\Gamma$  is the most relevant unknown in variational fracture problems and the theorems of Ambrosio [6], valid in particular for Griffith's type VF and global minimization, ensure that  $\Gamma$  is sufficiently regular to be approximated by sets composed by regular arcs, such as line elements. Therefore  $\Gamma$  is a 1d closed set and the unit normal  $\mathbf{n}$  and tangent  $\mathbf{t}$  exist a.e. along it.

The jump of  $\mathbf{u}$  across  $\Gamma$ , denoted  $[[\mathbf{u}]] = \mathbf{u}^+ - \mathbf{u}^-$ , is resolved into two components relative to  $\mathbf{n}, \mathbf{t}$

$$[[\mathbf{u}]] = a\mathbf{n} + b\mathbf{t} \quad (1)$$

The usual sign convention for discontinuities is such that if  $a$  is positive the corresponding points on the two opposite sides of the interface  $\Gamma$  separate and determine a vacancy. Therefore, to avoid interpenetration the following constraint on  $a$  must be considered:

$$a \geq 0$$

Finally we assume that  $\mathbf{u}$  belongs to  $H^1(\Omega \setminus \Gamma)$ , that is  $\mathbf{u}$  has the regularity required in linear elasticity away from  $\Gamma$ .

### Variational Fracture

The key assumption of the theory of brittle solids is that the material besides having an elastic energy density  $\varphi$  (bulk or volume energy in 3d) defined over  $\Omega \setminus \Gamma$  and depending on  $\varepsilon(\mathbf{u})$ , possesses an interface energy  $\theta$  (surface energy in 3d) defined over  $\Gamma$  and depending on  $[[\mathbf{u}]]$ . In VF, fracture nucleation and propagation is determined by minimization of the energy

$$E(u, \Gamma) = \int_{\Omega/\Gamma} \varphi(\varepsilon(u)) dx + \int_{\Gamma} \theta([[u]]) ds \quad (2)$$

Irreversibility of fracture requires that the set  $\Gamma(t+\Delta t) \supseteq \Gamma(t)$  for any time  $t$  and for any  $\Delta t > 0$ . This condition forces to consider an incremental formulation even if the loading is considered as quasi-static (quasi-static evolution). The main difference between static and dynamics is that in the first case the functional defined in (2) is the one to be minimized at any time  $t$ ; in the second case the evolution is ruled by the Euler equation of the functional

$$L(u, \dot{u}, \Gamma) = \frac{1}{2} \int_{\Omega/\Gamma} \rho \dot{u} \cdot \dot{u} dx = E(u, \Gamma) \quad (3)$$

### Volume and surface energy densities

The material is assumed to be elastic and isotropic, that is characterized by the elastic energy density, defined over  $\Omega \setminus \Gamma$ :

$$\varphi = \frac{1}{2} \lambda (\pi \varepsilon)^2 + \mu \varepsilon \cdot \varepsilon \quad (4)$$

The usual form of interface energy associated to Griffith's type brittle fracture is the following

$$\int_{\Gamma} \theta([[u]]) ds = \int_{\Gamma} G_c ds \quad (5)$$

where  $G_c$  is the so called surface fracture energy. We prefer to give to the interface energy density a more detailed form, accounting explicitly for sliding effects and including the constraint of non-interpenetration ( $a$  non negative):

$$\theta = \begin{cases} 0 & , a=0 \ \& \ b=0 \\ G_c' & , a=0 \ \& \ b \neq 0 \\ G_c & , a > 0 \\ +\infty & , a < 0 \end{cases} \quad (6)$$

equivalent to the form (5) if  $G'_c = G_c$  and the unilateral constraint on  $a$  is added to the energy minimization. By considering the constant  $G'_c$  lesser or greater than  $G_c$ , cases of materials for which sliding is more or less favourable can be considered.

## FE APPROXIMATION

### Space discretization

To discretize the problem we split the domain  $\Omega$  into constant strain triangles, as shown in Fig. 1, and identify  $\Gamma$  with the skeleton of the triangulation. The size of the mesh, that is the characteristic dimension of the smallest triangle, is denoted “ $h$ ”. In order to allow for discontinuous displacements we duplicate all the nodes and edges of the skeleton of the mesh, by introducing special interface elements with zero thickness placed along the edges of the finite elements.

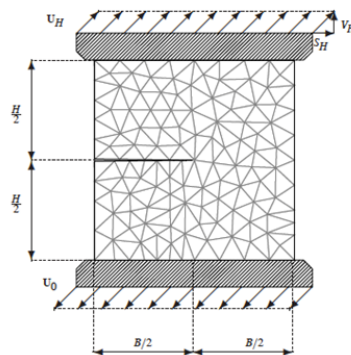


Figure 1: Discretization of the domain for a typical BVP .

In order to accurately approximate the location of cracks, our mesh is made variable in the sense that node positions in the reference configuration of the body are considered as further variables, then each node “ $i$ ” of the mesh has four degrees of freedom,  $x_1(i)$ ,  $x_2(i)$ ,  $u_1(i)$ ,  $u_2(i)$ , that is the coordinates of the node in the reference configuration and the components of the nodal displacement.

The elastic energy density  $\varphi(\varepsilon(\mathbf{u}))$ , written as a function of the node displacement  $\mathbf{u}(i)$  and of the reference coordinates  $\mathbf{x}(i)$  is carried by the triangular elements (linear, constant strain, elements) whereas on the interface elements the energy described in the following is defined. Notice that the use of triangular elements is compulsory if we want to make explicit the dependence of the energy on node positions.

### Energy relaxation

In the numerical applications we approximate the equilibrium trajectory of the system by considering crack propagation as based on critical points of the energy. To get out of possible small energy wells, either numerical (due to the finite element approximation) or physical (due to fracture initiation), we adopt a (mesh dependent) relaxed form of the surface energy density (6).

On introducing the limit tensile stress  $\sigma^0$ , the limit shear stress  $\tau^0$ , the shear stiffness  $k$  and the functions  $\theta_1(a)$ ,  $\theta_2(b)$

$$\theta_1(a) = G_c + \frac{2 G_c}{\pi - 2} \left( e^{\frac{a \psi \sigma^0}{G_c}} - 2 \text{ArcTan} \left( e^{\frac{a \psi \sigma^0}{G_c}} \right) \right) \quad (7)$$

$$\theta_2 = G'_c \left| \frac{b}{\sqrt{b^2 + \varepsilon^2}} \right| + \frac{2 \tau^0}{k \pi^2} \left( k \pi b \text{ArcTan} \left( \frac{k \pi b}{2 \tau^0} \right) - \tau^0 \text{Log} \left( 1 + \left( \frac{k \pi b}{2 \tau^0} \right)^2 \right) \right) \quad (8)$$



where  $\varepsilon$  is a smoothing parameter ( $\varepsilon=10^{-2} h \sim 10^{-4} h$ ,  $h$ : mesh size) and

$$\psi = \frac{2 - \pi}{\sqrt{2(5\sqrt{5} - 11)}}$$

the relaxed interface energy is defined as follows:

$$\theta(a,b) = \theta_1(a) + e^{-\tau a} \theta_2(b) \quad (9)$$

The plots of the two “components” of the relaxed interface energy are depicted in Figs. 2 a, b, for some special values of the parameters. In Fig. 2c the stress displacement relation on the interface corresponding to the surface energy represented in Fig. 2a is reported.

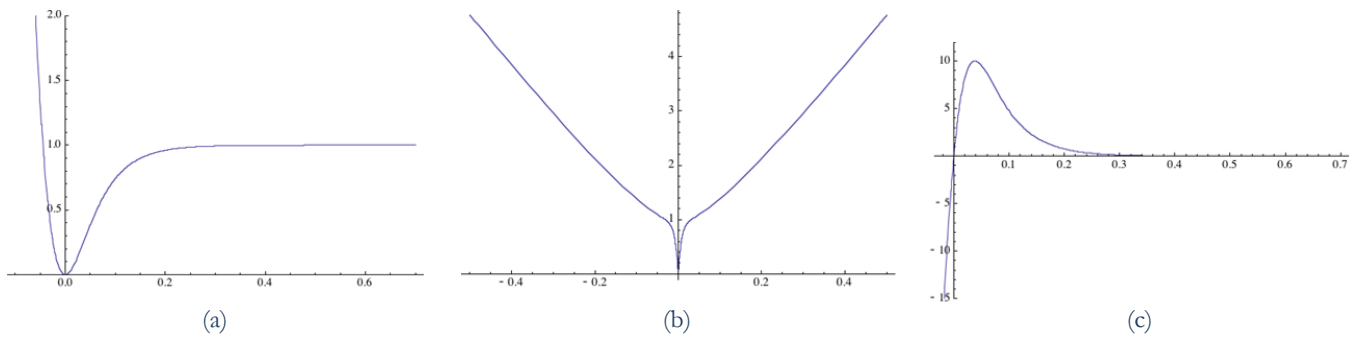


Figure 2: Plot of the interface energies  $\theta_1$ ,  $\theta_2$  as a function of  $a$  and  $b$  for  $G_c=1$ ,  $G'_c=1$ ,  $\sigma^o=10$ ,  $\tau^o=10$ ,  $k=100$ ,  $\varepsilon=0.01$ . In (c) the stress  $\sigma$  over the interface is plotted versus the jump  $a$ . The displacement jumps  $a$  and  $b$  are normalized with respect to  $h$ .

### Time discretization

We restrict to displacement BVP and assume that the data given on the constrained part  $S^1$  of the boundary is assumed to be time dependent. The time interval  $T$  is discretized into  $n$  time steps  $\delta$

$$t^i = i \delta, \quad i \in \{0, 1, \dots, n\} \quad (10)$$

At any loading step  $t^i$ , minimal states of the energy (2) are searched through an iterative descent procedure that uses as starting point the state at the previous step. Hence at any time step we look for a local minimizer, “accessible” from the previous step.

In particular, if a crack opens up at the step  $t^i$ , it is maintained at any step  $t^j$ ,  $j > i$ . This is done by making it a piece of the boundary that is setting over there the fracture energy thresholds  $G_c=G'_c=0$ . Notice that the shear part of the interface energy is maintained on such internal boundary (Cfr. the expression (8)) and a penalty term, depending on  $a$ , is added to avoid interpenetration in case of a successive self-contact.

## NUMERICAL EXPERIMENTS

### Propagation in mixed mode: initially uniform mesh.

In previous papers the 1d case, the validation with 2d Classical Linear Fracture Mechanics were presented (see [7], [8]). The Effect of mesh refinement in mixed modes I & II, was considered in [9]. A typical result of these numerical experiments, referring to mixed mode crack propagation (see Fig. 1) with  $S_H=-0.0005 L$ ,  $S_V=0.0005 L$  and adopting the geometrical and material data listed in Tabs. 1, 2, is reported in Fig. 3.

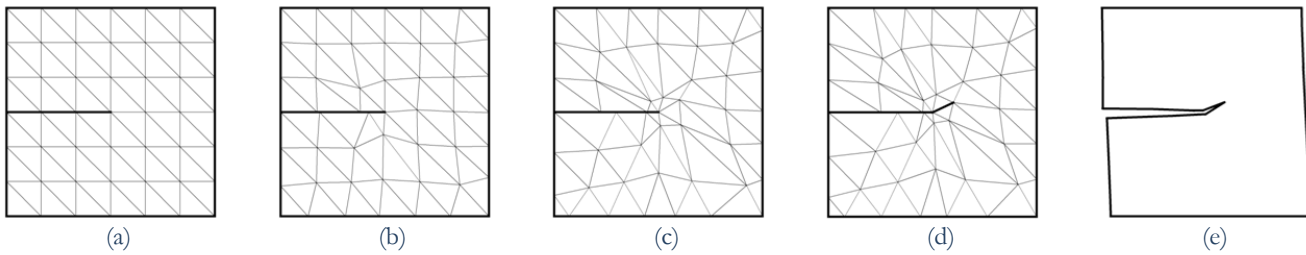


Figure 3: Propagation in mixed mode (see Fig. 1) with  $S_H = -\lambda 0.0005 L$ ,  $S_V = \lambda 0.0005 L$ . From (a) to (d) mesh at minimum state for  $\lambda = 0, 0.1, 0.4, 0.9$ . In (e) deformed shape after propagation; displacements are amplified 10 times.

The mesh considered in Fig. 3, uniform in the initial reference geometry, is rather coarse,  $h=0.0976 L$ , but an aspect that is common to all other examples where finer and finer mesh sizes were considered can still be observed: as the given displacement at the bases is gradually increased, before the final critical point (that is the step of loading at which the crack propagates) is reached, the elements around the tip of the pre-existing crack rearrange in a sort of star shaped pattern. The shape of the triangles that form the “star” tends to become hill shaped, that is extremely elongated in one direction. Actually the annihilation of such triangles in one direction is prevented because we put a lower bound to the least dimension of the triangles at each step of the evolution. In other words the minimization at each step of the loading process is performed adding this constraint on the mesh size  $h$ . We need to add this constraint (that prevent annihilation) since the parameters controlling the interface energy (see (7), (8), (9)) depend on mesh size. In the pictures (a)-(d) of Fig. 3 the displacement is proportionally increased from 0 to the final value and the following lower bounds for  $h/L$  are considered: 0.0976, 0.0488, 0.0244, 0.0122. The number of iterations necessary to obtain a satisfying minimum, increase dramatically as the critical point is approached (from the order of  $10^2$  to the order of  $10^4$ ).

In Fig. 4, where  $h=0.0586 L$  initially and  $h=0.00654$  at the limit point, the same pattern around the tip can be observed.

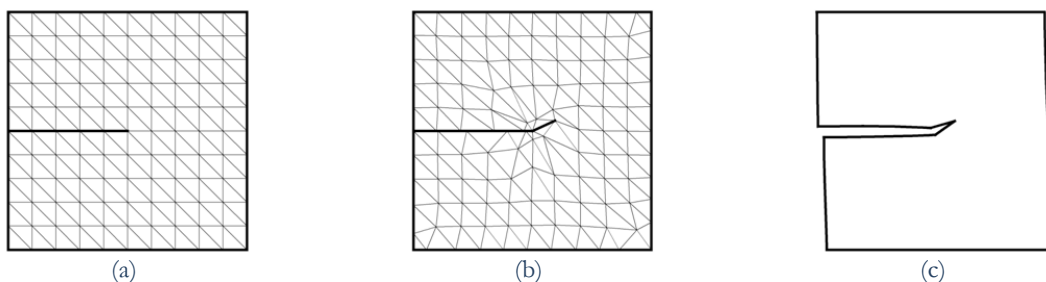


Figure 4: Propagation in mixed mode with  $S_H = -\lambda 0.0005 L$ ,  $S_V = \lambda 0.0005 L$ . In (a)  $\lambda = 0$  and in (b)  $\lambda = 0.84$ . In (c) deformed shape after propagation: displacements are amplified 10 times.

A non-uniform initial mesh is considered in Fig. 5 which refers to the boundary data of Fig. 1 with  $S_H=0.001 L$ ,  $S_V=0.001 L$ . The minimization steps shown in Fig. 5 are ordered on the base of the total number of iterations. A similar star shaped pattern of elements around the crack tip can be seen to appear before crack propagation.

#### *FE approximations and radical meshes: rate of convergence*

As we said our method works only with constant strain triangular elements and it is well known that with uniform meshes an  $r^\alpha$  singularity with  $0 < \alpha < 1$  (the type of singularity seen at reentrant corners:  $\alpha=1/2$  for slit cracks) yields no better than  $O(h^\alpha)$  convergence for the usual  $H^1$  variational formulation (see e.g. [10-18]).

The number of unknowns we can manage, in terms of computer time, with our approach is still rather low considering the  $O(h^{1/2})$  convergence, but there is a point we must consider.

To approximate the very large displacement gradients arising at the crack tip an extreme refinement of the mesh is required to achieve an acceptable convergence rate. For  $H^1$  methods it is known that graded mesh refinement can be used to recover the optimal convergence rate. Polynomials of degree  $p$  with radical meshes (see [10]) yield full  $O(h^p)$  convergence with  $H^1$  schemes (see also [11]). Radical meshes are meshes that are refined toward a boundary point by mapping a uniform mesh (see [12].) This is illustrated in Fig. 6 where a radical mesh over a rectangle  $\{0,1\} \times \{0,1\}$  is



obtained as the image of a uniform mesh under the map  $x \rightarrow x ||x||^{-1+1/(1-\mu)}$ .

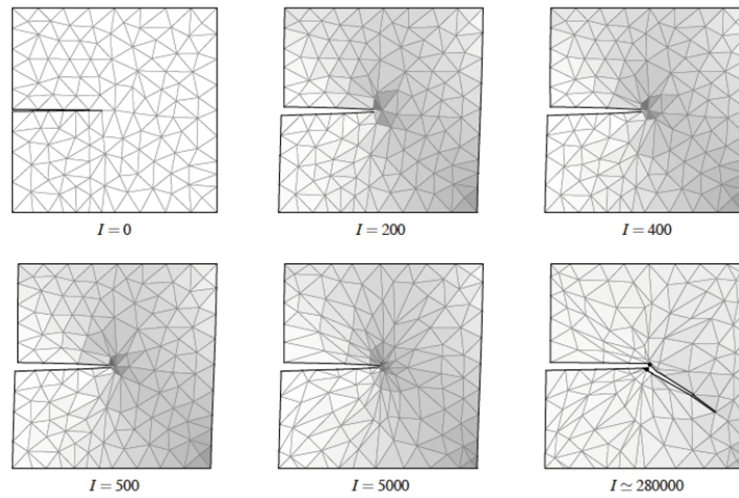


Figure 5: Propagation in mixed mode with  $S_H = -\lambda 0.001 L$ ,  $S_V = \lambda 0.001 L$ . In the first picture  $\lambda = 0$  and in the last  $\lambda = 1$ . The deformed shape is amplified 5 times.

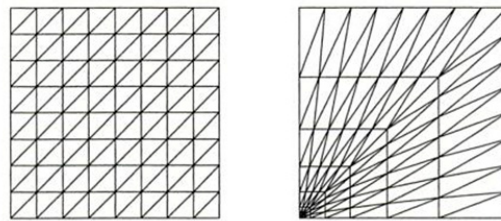


Figure 6: Radical mesh in a rectangle for  $\mu=2/3$ .

The star shaped pattern obtained as a result of our minimization process resembles closely that of a radical mesh with  $\mu=2/3$ , that is the one that is considered optimal, in the aforesaid class, for L shaped domains (Fig. 7). This suggests that the elongated triangles originating from the crack tip and obtained through energy minimization are optimal for the kind of approximation considered (constant strain triangles).

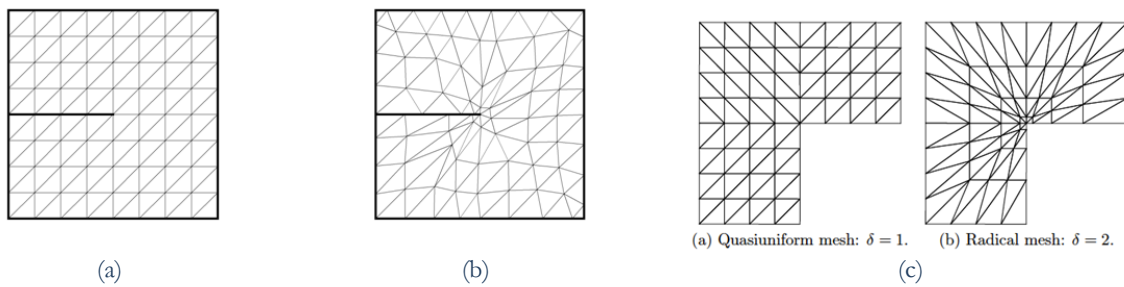


Figure 7: original uniform mesh with mesh size  $H=0.0732 L$  (a) and final optimized mesh at critical point (b) compared with a radical mesh for an L shaped domain with  $\mu=2/3$  (c).

*Propagation in mixed mode and nucleation: effect of the parameter  $\sigma^\circ$  for  $G_c = G'_c$ , and  $\tau^\circ$  large*

In this Subsection we address the problem of the dependence of our numerical results about crack propagation on the relaxation parameter  $\sigma^\circ$ . To this end we fix  $G'_c = G_c$  and assume a large value for the shear limit:  $\tau^\circ=10^4$ .

In the first example we consider the effect of the parameter  $\sigma^\circ$  for the mixed mode case of Fig. 1 with  $S_H=0.001 L$ ,  $S_V=0.001 L$ , and adopting the geometrical and material data listed in Tabs. 1, 2. The original mesh we consider is the non-

uniform mesh depicted in Fig. 1 and the results of the analysis for  $\sigma^0 = 100 \text{ N/cm}^2$  where those already shown in Fig. 5. By keeping all the other parameters fixed as in Tabs. 1, 2 and changing  $\sigma^0$  the results change sensibly. For  $\sigma^0 = 1000 \text{ N/cm}^2$  no propagation is detected. For lower values of the parameter the cracks start to diffuse all over the domain. The results of the analysis for  $\sigma^0 = 1 \text{ N/cm}^2$ ,  $\sigma^0 = 10 \text{ N/cm}^2$  and  $\sigma^0 = 100 \text{ N/cm}^2$ , are reported in Fig. 8 for comparison.

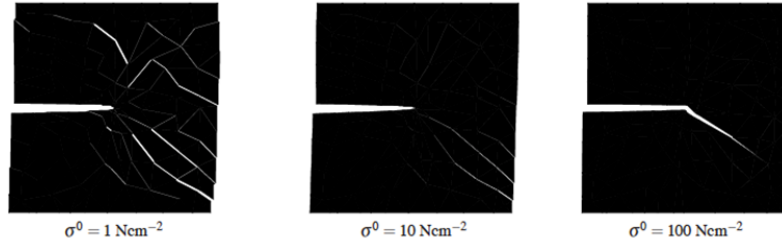


Figure 8: Example1, effect of the parameter  $\sigma^0$  on the crack propagation for the mixed mode case of Fig. 1.

In the second example we consider the effect of the parameter  $\sigma^0$  for the problem of fracture nucleation relative to the BVP shown in Fig. 9, with  $S_H = 0.0007 B$ ,  $S_V = 0.0007 B$ , and adopting the geometrical and material data listed in Tabs. 3, 4. The original mesh we consider is the uniform mesh depicted in Fig. 9. By keeping all other parameters fixed as in Tabs. 3, 4 and changing  $\sigma^0$  the results change sensibly. For  $\sigma^0 = 10^4 \text{ N/cm}^2$  no propagation is detected. For lower values of the parameter the cracks start to diffuse all over the domain. The results of the analysis for  $\sigma^0 = 1 \text{ N/cm}^2$ ,  $\sigma^0 = 10 \text{ N/cm}^2$  and  $\sigma^0 = 100 \text{ N/cm}^2$ , are reported in Fig. 10 for comparison.

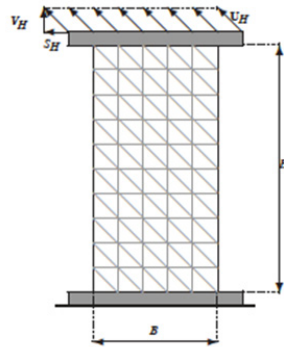


Figure 9: Discretization and boundary data for the second example.

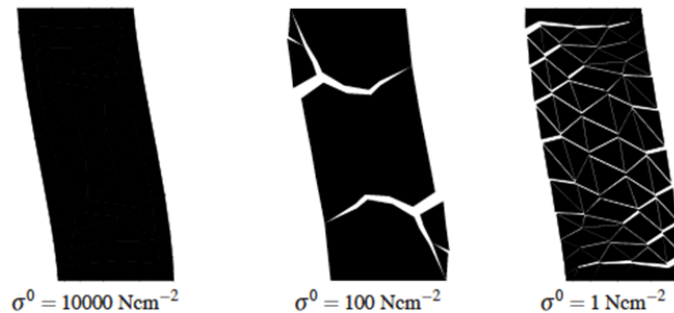


Figure 10: Example2, effect of the parameter  $\sigma^0$  on the crack propagation for the mixed mode case of Fig. 9.

*Nucleation in mixed mode: effect of the parameter  $\tau^0$ , for small  $G_c$  and large  $\sigma^0$*

In this Subsection we address the problem of the dependence of our numerical results about crack propagation on  $G_c$  and on the relaxation parameter  $\tau^0$ . To this end we fix  $\sigma^0 = 1000 \text{ N/cm}^2$ ,  $G_c = 0.01 G_c$  and assume a small value for the shear limit:  $\tau^0 = 10$ .





In the examples 3-5 we consider the case of Fig. 9 with  $\{S_H= 0.001 B, S_V=0\}$ ,  $\{S_H= 0.000924 B, S_V=0.000383 B\}$ ,  $\{S_H= 0.000707 B, S_V=0.000707 B\}$ , adopting the geometrical and material data listed in Tabs. 3, 4. The original mesh we consider is the uniform mesh depicted in Fig. 9. Due to the extreme weakness in shear of the material we expect that the minimal energy state in this three cases is a straight crack with slopes: 0,  $\frac{1}{2}$  and 1 respectively. This is the global minimum of the problem in the variational fracture frame for all three cases.

The results of the analysis are summarized in Figs. 11-13 by reporting the optimized mesh in the reference configuration at 6 stages of the loading process. In particular it is seen the elements in the reference configuration distort and change their shape in the reference configuration as the “load” is increased, but finally, an almost straight interface is detected. The slopes of the interfaces are exactly 0,  $\frac{1}{2}$  and 1. Notice that the crack is formed only at the last step: the solid line representing the final crack is reported for tracking the evolution of the interface during the loading process.

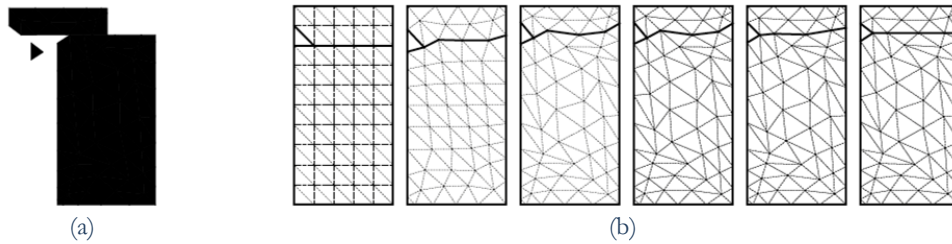


Figure 11: Example 3, crack nucleation for a brittle material weak in shear: BVP of Fig. 9 with  $S_H= 0.001 B, S_V=0$ .

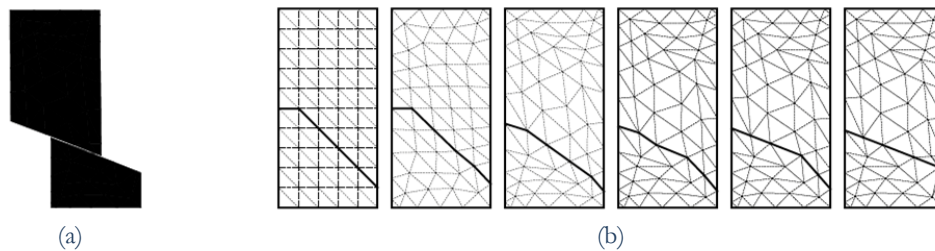


Figure 12: Example 4, crack nucleation for a brittle material weak in shear: BVP of Fig. 9 with  $S_H= 0.000924 B, S_V=0.000383 B$ .

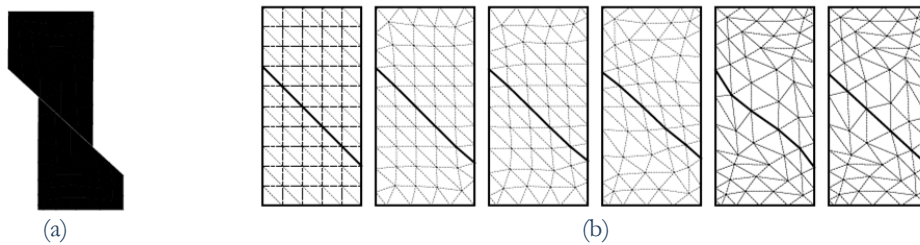


Figure 13: Example 5, crack nucleation for a brittle material weak in shear: BVP of Fig. 9 with  $S_H= 0.000707 B, S_V=0.000707 B$ .

In the last example we try to assess the effect of the variation of the mesh in the elastic phase, by fixing the nodes in the reference configuration during the elastic evolution (that is before the critical point) and allowing for mesh variation only at the last step. The same data of example 3 are considered but in this the solution obtained at the end consists of two cracks instead of one, that is the system evolves to an equilibrium state of fracture that is only a local minimum.

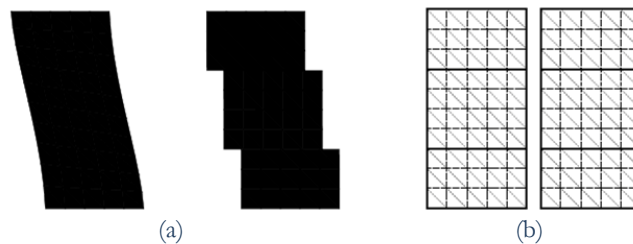


Figure 14: Example 6, crack nucleation for a brittle material weak in shear: BVP of Fig. 9 with  $S_H= 0.001 B, S_V=0$ . The mesh variation has been blocked in the “elastic” phase.



H (cm)	L (cm)	T, thickness (cm)	E, Young modulus (N/cm <sup>2</sup> )	$\nu$
10.0	10.0	1.0	3.0 10 <sup>5</sup>	0.0

Table 1: Geometric and material parameters for the example of Fig. 1.

$G_c$ (Ncm <sup>2</sup> )	$\sigma^\circ$ (N/cm <sup>2</sup> )	$\tau^\circ$ (cm) (N/cm <sup>2</sup> )	k (N/cm)
10.0	1.0, 10.0, 10 <sup>2</sup> , 10 <sup>3</sup>	1.0 10 <sup>4</sup>	1.0 10 <sup>5</sup>

Table 2: Material parameters for the interface energy relative to the example of Fig. 1.

H (cm)	L (cm)	T, thickness (cm)	E, Young modulus (N/cm <sup>2</sup> )	$\nu$
20.0	10.0	1.0	3.0 10 <sup>5</sup>	0.2

Table 3: Geometric and material parameters for the example of Fig. 9.

$G_c$ (Ncm <sup>2</sup> )	$\sigma^\circ$ (N/cm <sup>2</sup> )	$\tau^\circ$ (cm) (N/cm <sup>2</sup> )	k (N/cm)
10.0	1.0, 10 <sup>2</sup> , 10 <sup>5</sup>	1.0, 1.0 10 <sup>4</sup>	1.0 10 <sup>5</sup>

Table 4: Material parameters for the interface energy relative to the example of Fig. 9.

## CONCLUSIONS

In this paper we considered some benchmark problems concerning crack propagation in notched specimens and crack nucleation in sound specimens. The approach can be classified into the family of the discrete crack models. We consider special interface elements with zero thickness placed along the edges of the triangular elements and, since the crack location and orientation is not known in advance, we adopt variable meshes in order to allow for the skeleton of the mesh to adapt to optimal fracture patterns. Special attention is paid to the numerical implementation concerning crack path irreversibility. In particular the fracture process is discretized into steps and if a fracture opens up at a certain step, it is maintained at any successive step. The proposed method needs no assumptions on the crack geometry.

The results are encouraging but much has to be done. The results depend strongly on the choice of the relaxation parameters and, apart from very rough bounds, simple rules to set interface parameters have still to be found as well as a new strategy for more efficient ways to get out of the energy wells.

Although the restriction to constant strain triangles seems awkward on considering the strong stress singularity and the severe limitations we have on the node number, the method has the ability to adapt the mesh to its optimal shape (that is the best shape for the given node number). Very good results were obtained for brittle materials that are very weak in shear. The role of mesh adaptation in the elastic phase seems important in these cases.

## REFERENCES

- [1] R. Krueger, *Appl. Mech. Rev.*, 57 (2) (2004) 109.
- [2] N. Moes, J. Dolbow, T Belytschko, *Int. J. Num. Meth. Eng.*, 46 (1) (1999) 131.
- [3] L. Ambrosio, V.M. Tortorelli, *Comm. Pure Appl. Math.*, 43 (8) (1990) 998.
- [4] C.J. Larsen, In: *IUTAM Symposium on "Variational Concepts with Applications to the Mechanics of Materials*, Springer-Netherlands, 21 (2010) 131.
- [5] M.J. Borden, C.V. Verhoosel, M.A. Scott, T.J.R. Hughes, C.M. Landis, Report 11, Institute for Computer Engineering and Science, University of Texas at Austin (2011).



- [6] Ambrosio, *Boll. Un. Mat. Ital.*, 3–B (1989) 857–881.
- [7] M. Angelillo, E. Babilio, A. Fortunato, *Mechanical Modelling and Computational Issues in Civil Engineering, Proc. Colloquium Lagrangianum (2001)*, Le Mont Saint Michel, France, Fremond and Maceri editors, Springer (2005).
- [8] M. Angelillo, E. Babilio, In: *Proceedings of XIII AIMETA Congress*, Ancona, Italy (2009).
- [9] M. Angelillo, E. Babilio, A. Fortunato, In: *Proc. CanCNSM*, Toronto, Canada (2008).
- [10] I. Babuska, T. Strouboulis, *Numerical Mathematics and Scientific Computation*, The Clarendon Press Oxford University Press, NewYork (2001).
- [11] T. Apel, A.M. Sandig, J. R. Whiteman, *Math. Methods Appl. Sci.*, 19 (1996) 63.
- [12] V. A. Kozlov, V. G. Mazya, J. Rossmann, *Elliptic boundary value problems in domains with point singularities*, vol. 52 of *Mathematical Surveys and Monographs*, American Mathematical Society, Providence, RI (1997).